IOPscience iopscience.iop.org

Home Search Collections Journals About Contact us My IOPscience

Optical processes in ZnO

This article has been downloaded from IOPscience. Please scroll down to see the full text article.

1995 J. Phys.: Condens. Matter 7 10029

(http://iopscience.iop.org/0953-8984/7/50/032)

View the table of contents for this issue, or go to the journal homepage for more

Download details:
IP Address: 171.66.16.151
The article was downloaded on 12/05/2010 at 22:47

Please note that terms and conditions apply.

J. Phys.: Condens. Matter 7 (1995) 10029–10036. Printed in the UK

Optical processes in ZnO

Michio Sasanuma
Department of Applied Physics, Osaka City University, Osaka 558, Japan

Received 22 May 1995, in final form 7 September 1995

Abstract. Interpretation of the optical processes in ZnO is presented. All the data on photon emission and absorption from the UV to the IR region are treated by a localized molecular unit model. Spectral assignments and characteristics of the shift of the emission band with temperature are interpreted by the present model.

1. Introduction

Optical processes in solids have been treated mainly by the band theory and the exciton effect. However, there remain some unsolved problems on the observed optical processes. For ZnO, fine structure in the UV emission band and the red shift of the spectrum with increasing temperature have been left unsolved in the exciton effect. Apart from the exciton model, the localized molecular unit model explains explicitly the observed results. For example, the ESCA spectra of TiO_2 are well assigned by a molecular orbital model [1]. The infrared reflectivity of amorphous silica is also explained by the molecular picture [2].

We examine optical processes in ZnO by the molecular model from an analysis of experimental data on photoemission and absorption. In the model, a photon interacts with a localized electron of an atomic orbital in a potential energy function $|x_i\rangle$. The $|x_i\rangle$ relates to the band wavefunction $|k\rangle$ of wavenumber k by the usual relation $|k\rangle = \sum_i \exp(ikx_i)|x_i\rangle$. The electronic and vibrational characteristics appearing in the photon absorption and emission processes reflect the changes in the potential energy functions.

The non-conducting excited state described in an old textbook [4] concerns the present picture. It differs completely from the picture of the exciton effect expressed by the Rydberg states and their couplings with phonon bands. We consider that the degenerate atomic ground state changes to independent energy states under the influence of a crystal field. For example, the $J = 2$, 1 and 0 states of the $(2p)^4\,{}^3P$ configuration of atomic oxygen contribute separately to the optical processes. These states are usually disregarded in the band-structure calculation.

In this paper we assign the emission and absorption fine structures and the shift of the spectrum for ZnO. The orange band observed at high temperatures is analysed in the scheme of the potential energy functions. The shift of the spectrum and intensity distributions of the orange band are calculated and compared with experiments.

2. General consideration

A general formalism has been given in [3]. We summarize the necessary part for the present analysis. The wavefunction of the ground state of ZnO is expressed as

0953-8984/95/5010029+08$19.50 © 1995 IOP Publishing Ltd

$|a, i\rangle \equiv |{}^1S_0(4s_{Zn})^2 + {}^3P_2(2p_O)^4\rangle|i\rangle$. $|a\rangle$ is a linear combination of the 4s atomic orbitals of the $^1S_0$ state of the zinc atom and 2p atomic orbitals of the $^3P_2$ state of an oxygen atom which make up the electronic state of the ZnO molecular unit. $|i\rangle$ represents the vibrational states associated with the potential energy function. The excited-state potential energy function associated with the vibrational state $|j\rangle$ is expressed as $|b, j\rangle \equiv |{}^1S_0(4s_{Zn})^2 + {}^5S_2([2p_O]^3[3s])\rangle|j\rangle$.

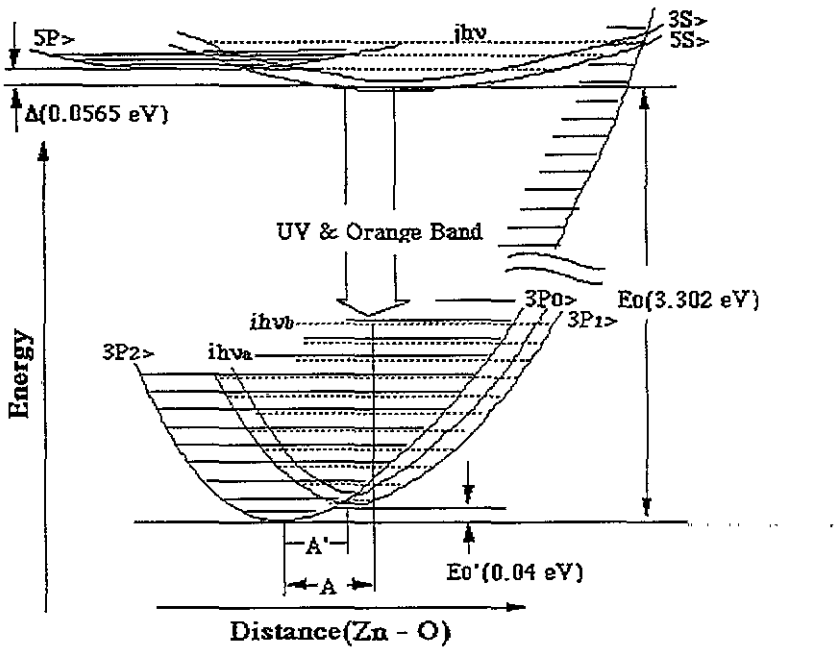

Figure 1. Schematic potential energy functions associated with the electronic states of an oxygen atom in ZnO. $^3P_2\rangle$ is the ground state associated with the vibrational states $|i\rangle$. $^5S_2\rangle$ and $^3S_1\rangle$ are the excited states. $^5P\rangle$ denotes the bottom of the conductive state. Transitions from $^5S_2\rangle$ to $^3P_{0,1,2}\rangle|i\rangle$ correspond to the UV and orange bands. Transitions from $^3P_{J'}\rangle$ to $^3P_J\rangle$, $(J, J' = 1, 2, 3, J \neq J')$ gives the IR band.

The schematic diagram of the potential energy functions of ZnO is shown in figure 1. The abscissa is the real distance between atoms that contribute to the potential energy function. The energy of the molecular state is the sum of orbital energies of the constituent atoms and the vibrational energy associated with the potential energy function. The condition for interaction between a photon of energy $h\nu$ and a molecular unit is $h\nu = E_0 + h\nu_b - h\nu_b$, where E_0 is the difference between the electron's orbital energies in the initial and the final states. ν_a and ν_b are vibrational energies associated with the potential energy functions of the initial (a) and final (b) states.

The potential energy function contributing to the electric current is a shallow excited potential of small coupling constant and it spreads outside the unit cell. The small vibrational energy looks continuous. The potential energy function from p symmetric wavefunctions in excited states are considered to be responsible for the electric current.

In the present treatment, we approximate the potential energy function by the harmonic potential of the breathing mode. A constant value for the energy difference between the fine structures of the UV emission band assures the harmonic potential for the ground-state potential [6]. The emission intensity for a photon of energy $h\nu$ at temperature T is expressed

as

$$I(a,b,h\nu,T) = h\nu \sum_{i,j}^{i_{max},j_{max}} N_0(j,T)\rho(i,T)|\langle b,j|R|a,i\rangle|^2\delta(h\nu - E_0 - jh\nu_b + ih\nu_a) \quad (1)$$

where $N_0(j,T) = \exp(-jh\nu_b/kT)\{1-\exp(-h\nu_b/kT)\}$ represents the probability that the system is in an initial vibrational state $|j\rangle$ of the excited-state potential energy function. The final-state density $\rho(ih\nu_a,T) = \exp(-ih\nu_a/kT)\{1-\exp(-h\nu_a/kT)\}$ is related to the probability for the vibrational state $|i\rangle$ in the ground-state potential energy function. $|\langle b,j|R|a,i\rangle|^2 = |\langle b|P|a\rangle|^2|\langle j|i\rangle|^2$. $|\langle b|P|a\rangle|^2$ represents the electronic transition probability and is proportional to ν^3 in the electric dipole transition.

The vibrational transition associated with the electronic transition is expressed by

$$|\langle j|i\rangle|^2 = \sqrt{\{(\nu_b/\nu_a)/(\pi 2^{i+j}i!j!)\}}\left|\int \exp[-\tfrac{1}{2}(\nu_b/\nu_a)(r-A)^2 + r^2]H_i(r)H_j(r-A)\,dr\right|^2 \quad (2)$$

$A = 2\pi\sqrt{\{(m\nu_a)/h\}}x_0\}$, $r = 2\pi\sqrt{\{(m\nu_a/h)x\}}$ and x_0 is the distance between the two potentials in the equilibrium position. ν_a and ν_b are the fundamental frequencies in the ground- and excited-state potential energy functions. δ is the delta function for describing the energy conservation in the transition. E_0 is the energy difference between the two states. m is the reduced mass of the molecular system of the potential energy function.

Equation (1) is easily calculated in the harmonic potential approximation.

3. Analysis of ZnO UV data

We can explain all the UV absorption and emission data in our scheme. We adopt the absorption data of Liang and Yoffe [6] and the emission spectra obtained by Mollwo and co-workers [5,7].

By the present model, the electronic ground state is the triply degenerate states ($J = 2, 1, 0$) of oxygen 2p orbitals [8]. The contribution of the zinc 4s electron to the optical process in the UV region does not exist. The green band of emission observed in a zinc-rich sample is considered to reflect the transition of the zinc 4s electron [5]. The UV absorption structures of ZnO are assigned as the exciton series and their couplings with phonon modes [6]. We assign them as the electron transition from the states $|{}^1S_0(Zn) + {}^3P_J(O)\rangle|i\rangle$ ($J = 2$, 1 and 0) to the states $|{}^1S_0(Zn) + {}^{(2S+1)}L_J(O)\rangle|j\rangle$ in the present scheme. Here S, L and J are the spin, orbital and total angular momentum quantum numbers, respectively. The ratio of about 0.6 of the absorption intensity for $n = 2$ to that for $n = 1$, assigned as the exciton states in figure 1 of [6], reflects the final-state densities of ${}^5S$ and ${}^3S$ states. The energy sequence ${}^5S$, ${}^3S$, ${}^5P$ of atomic oxygen is considered to be maintained in the ZnO molecular unit [8]. As is seen in figure 2, the structures $L_{1a}(\perp,\|)$, $L_{1b}(\perp,\|)$ and $L_{2a}(\perp,\|)$, $L_{2b}(\perp)$ of [6] are assigned as the transitions from the $i = 0$ state of three $|{}^3P\rangle$ to the $J+1$ and 2 states of $|{}^1S_0(Zn) + {}^5S_2(O)\rangle$. L_{1b} and L_{2b} in $E\|c$ are assigned as another vibrational mode associated with $|{}^1S_0(Zn) + {}^3S_1(O)\rangle$. The energy differences of the absorption structures are classified into groups as shown in table 1. These give the energy gaps of the potential energy functions. The broadening and shift of the absorption edge observed in [6] are solved by evaluating equation (2).

The UV emission spectra involve fine structure with an energy difference of about 0.07 eV in the energy region 3.302–3.027 eV [5,7]. We assign them as a vibrational progression of the transitions from the state $|{}^1S_0(Zn) + {}^5S_2(O)\rangle|j = 0\rangle$ to the state

Table 1. Energies (eV) between the terms are obtained from the scheme in figure 1. The terms are labelled using the configuration of the oxygen atom.

$^3P_2$–$^3P_1$	$^3P_1$–$^3P_0$	$^3S_1$–$^5S_2$	^5P–$^3S_1$	$^5S_2(j=1)$–$^5S_2(j=0)$	$^5S_2(j=2)$–$^5S_2(j=1)$	$\Delta(^5P$–$^5S_2)$
$C_1 - B_1$, 0.0408	$B_1 - A_1$, 0.0075	$A_2 - A_1$, 0.0501	$A_3 - A_2$, 0.0093	$L_{1a}(\perp) - A_1(\perp)$, 0.0699	$L_{2a}(\perp) - L_{1a}(\perp)$, 0.063	$A_3 - A_1$, 0.0594
$C_2 - B_2$, 0.0398	$B_2 - A_2$, 0.0042	$B_2 - B_1$, 0.0468	$B_3 - B_2$, 0.0088	$L_{1a}(\perp) - B_1(\perp)$, 0.0784	$L_{2b}(\perp) - L_{1b}(\perp)$, 0.061	$B_3 - B_1$, 0.0551
$C_3 - B_3$, 0.0396	$B_3 - A_3$, 0.0037	$C_2 - C_1$, 0.0458	$C_3 - C_2$, 0.0086	$L_{1a}(\parallel) - C_1(\parallel)$, 0.0656	$L_{2a}(\parallel) - L_{1a}(\parallel)$, 0.061	$C_3 - C_1$, 0.0544
					$L_{2b}(\parallel) - L_{1b}(\parallel)$, 0.068	
0.0401	0.0051	0.0476	0.0089	0.0713	0.063	0.0565

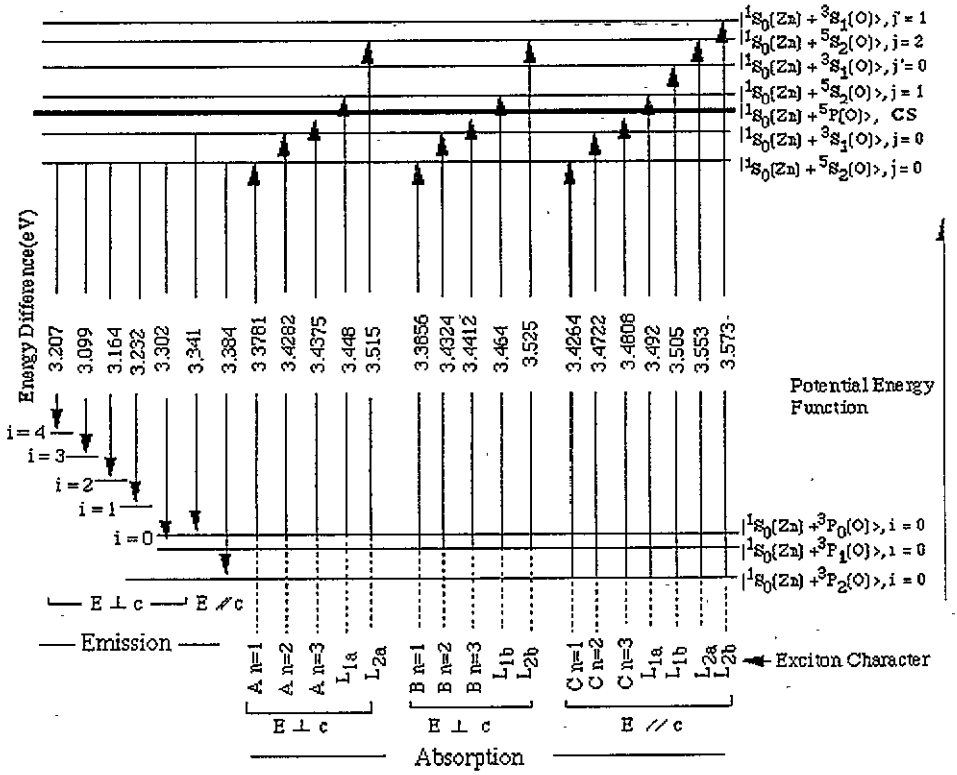

Figure 2. Energy levels are assigned by the absorption and emission data of ZnO. Horizontal lines correspond to the energy levels of potential energy functions. The vertical arrow show the transitions and energy difference between the states. cs denotes the bottom of the conductive state ^{5}P). The numerical values are the experimental data in electronvolts. Analysis of the absorption structures obtained by the exciton effect are compared in the lower part of the figure.

$|^1S_0(Zn) + {}^3P_{0,1}(O)\rangle|i = 0, 1, 2, 3, 4\rangle$. The ground-state potential energy functions $^3P_1\rangle$ and $^3P_0\rangle$ are close together, 0.0051 eV (table 1). The UV fine structures may involve both transitions to these final states. The intense emission band at 3.341 eV is identified as the 0–0 transition from the state $|^1S_0(Zn) + {}^3S_1(O)\rangle$ to the state $|^1S_0(Zn) + {}^3P_0(O)\rangle$. The weak 3.384 eV band of polarization parallel to the c axis is identified as the transition $|^1S_0(Zn) + {}^5S_2(O)\rangle|j = 0\rangle \rightarrow |^1S_0(Zn) + {}^3P_2(O)\rangle|i = 0\rangle$. The state $|^1S_0(Zn) + {}^5P(O)\rangle$ is assigned as the conductive state. Electrons in the p symmetry state in the excited state will contribute to the electric current. The continuous feature of the absorption structure beyond 3.4412 eV reflects this [6]. Heiland *et al* [5] and Nicoll [9] observed a decrease in UV emission intensity and a shift to long wavelength with increasing temperature. It can be interpreted as a loss of the excited-state density by the non-radiative transition from $|^1S_0(Zn) + {}^5S_2(O)\rangle|j\rangle$ to $|^1S_0(Zn) + {}^5P(O)\rangle$ for the energies above Δ (figure 1). The emission intensity $I(T)$ at temperature T is proportional to the probability for which the thermal distribution of the vibrational states is in an effective potential of depth Δ. It is estimated from the following equation:

$$I(T) = \left(\int_0^{\Delta} \frac{-E}{kT} \mathrm{d}E\right) \Big/ \int_0^{\infty} \left(\frac{-E}{kT} \mathrm{d}E\right). \tag{3}$$

We obtain $\Delta = 0.054$ eV from the UV data [5]. It corresponds to the energy difference

of 0.0565 eV between the states of $|{}^1S_0(Zn) + {}^5P(O)\rangle$ and $|{}^1S_0(Zn) + {}^5S_2(O)\rangle|j = 0\rangle$ in table 1. The broad absorption structure of L_{1a}, etc, is due to the autoionization of the quasi-bound state $|{}^1S_0(Zn) + {}^5S_2(O)\rangle|j = 1, 2\rangle$, etc, to the continuous state.

The decreases in the vibrational band gap of j and j' progressions show the anharmonic character of the excited-state potential energy functions. They constitute the different vibrational modes of $|{}^1S_0(Zn) + {}^3S_1(O)\rangle$ shown in figure 2. An assignment for the transition in figure 2 corresponds to all the combinations involving the spin-flip transitions. It is due to the perturbation of the crystal field due to electron transitions.

4. Temperature shift of the spectrum (orange band)

The orange band of ZnO is assigned using the same scheme of the electronic transitions as for the UV emission. The excitation to the $|{}^1S_0(Zn) + {}^5S_2(O)\rangle|j = 0\rangle$ state is attained by heating. It induces the probability distribution of the vibrational level at large i of $ih\nu_a \geqslant E_0$ in the ground-state potential energy function $|{}^1S_0(Zn) + 3P_2(O)\rangle|i\rangle$ (figure 1). The probability of thermal distribution, $\exp(-E_0/kT)$, is about 10^{-12}, for $E_0 \approx 3$ eV and $T \approx 1000\,°C$. At this temperature, the numbers of the excited states in a sample volume of 10^{-2} cm $\times$ 1 cm^2 is approximately $10^{-12} \times 10^{23} \times 10^{-2} = 10^9$, which distributes at the ith vibrational levels of $i \approx 3.0/0.07 \approx 43$ and makes a possible transition to the electronic excited states, $|{}^5S_2(O)\rangle$ or $|{}^3S_1(O)\rangle$.

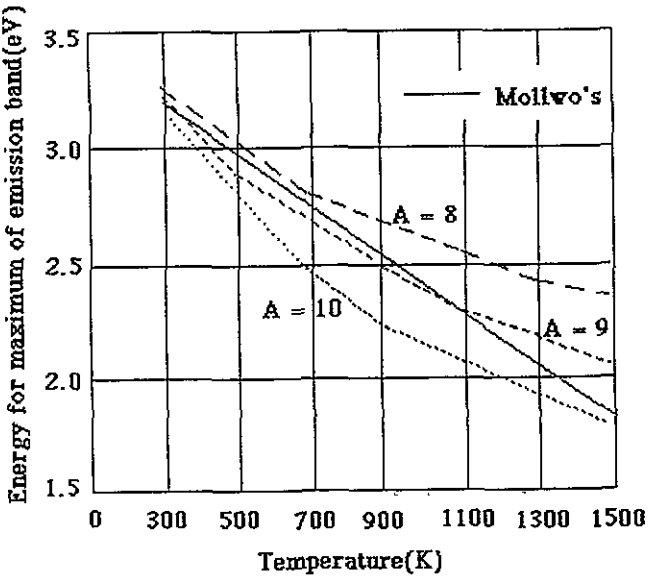

Figure 3. Position of the maximum of the emission band as a function of temperature calculated for parameter A and compared with analysis of the experimental data by Mollwo and co-workers.

The energies for the maximum of the spectral distribution are obtained from equation (2) and the results for the temperatures from 300 to 1500 K are shown in figure 3. The experimental parameters $E_0 = 3.302$ eV and $h\nu_a = h\nu_b = 0.07$ eV and the presupposed values $i_{max} = 40$ and $j_{max} = 1$ are used in the calculations. The unknown parameter A is selected for the calculated temperature coefficient to match the experimental value. The result for $A = 9$ approaches the experimental value of -11.5×10^{-4} eV K^{-1}. In figure 4, the

calculated relative intensity profiles near the maximum of the emission band are compared with the experimental profiles at room temperatures of 870–1090 °C [5].

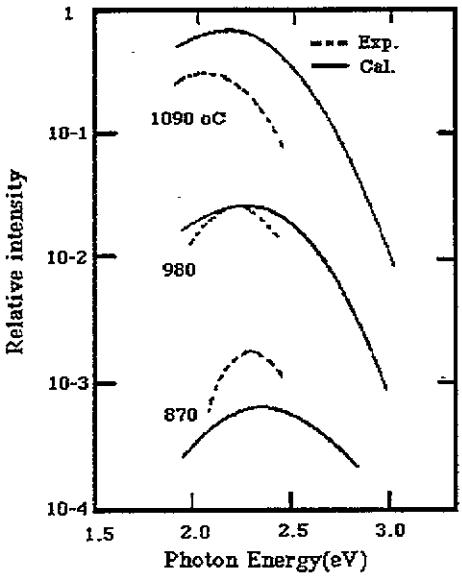

Figure 4. Calculated relative spectral emission intensities of the orange band at different temperatures compared with experimental data. In the calculations, the vibrational energies of potential energy functions are taken as 0.07 eV and the energy difference between ^5S) and $^3P_2$) is taken as $E_0 = 3.302$ eV. The parameter A is chosen to fit the experimental result.

The calculated spectrum is broad compared with the experimental spectrum. The difference is considered to be due to the following. The observed spectral distribution in figure 4 is the sum of the profiles induced by the transitions from the potential energy functions of the excited states $^3S_1$) and $^5S_2$) to those of the ground state ^3P_J) ($J = 0, 1, 2$). The calculation is done for one transition. When we try more careful calculations choosing parameters on potential shapes ($m\omega_a^2$) and distance (A), some different results may be expected.

We can expect a breathing mode for the ground-state potential energy function extended to the excited electronic state (figure 1) . This gives rise to thermal excitation of an electron in the ground state to the excited state. The orange band is induced by this process. It is an inverse electronic process as against the non-radiative relaxation of photon absorption. Electron transitions between harmonic potentials give a common temperature coefficient as is shown for the UV and orange band (figure 3). It shows good harmonicity of the ground-state potentials of ZnO.

5. Conclusion

The molecular model analysis gives reasonable results for the optical data of ZnO. It treats the photon interaction processes in solids as electron transitions between potential energy functions associated with vibrational states. From the assignment of figure 2, all types of transition, such as the electron's spin-flip transition, are possible under the effect of a crystal field.

The green band of ZnO, observed in a zinc-rich sample, shows no shift in its spectral

peak position and its intensity decreases under an applied voltage [6]. These phenomena can be interpreted by the molecular model. We consider the green band as the emission induced by an electron transition from ^3P to ^1S states of the zinc atom. The potential energy function associated with the ^3P state of the zinc atom is a localized wavefunction, but its form is expected to be shallow and extends to neighbouring unit cells. The 4p electron of the zinc atom will recombine to the ^1S state, emitting green light. Under application of an electric field, the 4p electron will drift along the applied field and the emission intensity will decrease.

An analysis of the mechanism of the orange band as radiative recombination of electron–hole pairs arising from thermal excitation does not give reasonable results for the recombination cross section and its temperature dependence [6]. We can check the model from experimental data on the emission intensity. The numbers of electron–hole pairs must be smaller than the photon number from thermal radiation in the same energy region. ZnO and TiO_2 show colouration bands with a strong intensity compared with the intensity of thermal radiation [10]. It is inconsistent with the model based on electron–hole pairs.

ESCA data for TiO_2 are well assigned as the transitions between molecular orbitals [1]. The temperature-dependent behaviours of the photocurrent and quantum yield of TiO_2 at around 3 eV have been reported [11]. These are also possible to interpret by the molecular model in the same manner as for ZnO. The doublet structure of the photocurrent profile corresponds to transitions from the ground electronic states [12]. In contrast with ZnO, the energy splittings are large and these appear in the structures of the quantum yields at lower temperatures.

The IR emission band of ZnO, usually treated as thermal radiation, can also be described by the transitions between the potential energy functions of the triplet states, ^3P_J) ($J = 2, 1, 0$) and the spectral profile can be found when we have obtained the parameters in calculations [3].

We may conclude that the molecular model is important in understanding the optical processes, and numerical results on the spectral profile and its shift can easily be obtained using this model.

References

[1] Fisher D W 1972 *Phys. Rev.* B 5 4219
[2] Laughlin R B and Joannopoulos J D 1977 *Phys. Rev.* B 16 2942
[3] Sasanuma M 1995 *J. Phys. Soc. Japan* 64 450
[4] Seitz F 1940 *The Modern Theory of Solids* (New York: McGraw-Hill) p 254
[5] Heiland G, Mollwo E and Stockmann F 1959 *Solid State Physics* vol 8, ed F Seitz and D Turnbull (New York: Academic) p 216
[6] Liang W Y and Yoffe A D 1968 *Phys. Rev. Lett.* 20 59
[7] Andrew B and Mollwo E 1959 *Naturwissenschaften* 22 628
[8] Moore C 1949 *Atomic Energy Levels (NBS Circular 467)* vol I (Washington, DC: US Government Printing Office) p 45
[9] Nicoll F H 1948 *J. Opt. Soc. Am.* 38 817
[10] Sasanuma M and Senda H 1995 *J. Phys. Soc. Japan* 64 1044
[11] Cronemeyer D C 1952 *Phys. Rev.* 87 876
[12] Sasanuma M 1955 *J. Phys. Soc. Japan* 64 3122